EFFECTS OF STATIC EQUILIBRIUM AND HIGHER-ORDER NONLINEARITIES ON ROTOR BLADE STABILITY IN HOVER

Marcelo R.M. Crespo da Silva*
and
Dewey H. Hodges**

Aeromechanics Laboratory
U.S. Army Research and Technology Laboratories (AVRADCOM)
Ames Research Center
Moffett Field, California

Abstract

The equilibrium and stability of the coupled elastic lead/lag, flap, and torsion motion of a cantilever rotor blade in hover are addressed, and the influence of several higher-order terms in the equations of motion of the blade is determined for a range of values of collective pitch. The blade is assumed to be untwisted and to have uniform properties along its span. In addition, chordwise offsets between its elastic, tension, mass, and aerodynamic centers are assumed to be negligible for simplicity. The aerodynamic forces acting on the blade are modeled using a quasi-steady, strip-theory approximation.

1. Introduction

An important problem in helicopter dynamics is the determination of the dynamic response and aeroelastic stability associated with the rotor blades. Considerable attention has been directed to rotary-wing aeroelasticity problems, and it is now widely recognized that such problems are inherently nonlinear. Hodges and Dowell[1] developed a comprehensive set of differential equations of motion, with quadratic nonlinearities, describing the flap-lead/lag-torsional dynamics of slender, rotating extensional rotor blades undergoing moderately large elastic deformations. An ordering scheme based on a small parameter ϵ was introduced in Ref. 1 to systematically neglect higher-order terms in the equations. Some important linear terms of order ϵ^3 were kept in the equations such as aerodynamic damping terms in the lead/lag and torsional differential equations and inertia terms in the torsional differential equation. Nonlinear terms of $O(\epsilon^3)$ were systematically neglected. The equations of motion developed in Ref. 1 were used in Ref. 2 to investigate the stability of the elastic motion of a uniform cantilever rotor blade in the hover flight condition.

A set of $O(\epsilon^3)$ nonlinear differential equations describing the flexural-flexural-torsional motion of inextensional beams undergoing moderately large deformations was derived by Crespo da Silva and Glynn and used by the same authors to analyze the response of the system[3]. They have considered nonrotating beams, and determined the effect of these nonlinearities on the response of the system for the cases in which the torsional frequencies of the beam are much larger than its bending frequencies. For such cases, the nonlinearities present in the differential equations of motion are $O(\epsilon^3)$ rather than $O(\epsilon^2)$.

The question that immediately arises for the rotating rotor-blade problem is whether cubic nonlinearities can also play a significant role in the equilibrium and stability of the elastic motion of the blade. To address this question, the differential equations, and their boundary conditions, describing the flap-lead/lag-torsional elastic motion of a rotor blade were derived in Ref. 4 with the objective of retaining in the equations all the nonlinear terms up to $O(\epsilon^3)$ in a small parameter ϵ. The equations developed in Ref. 4 extend those developed in Ref. 1 to include not only all linear $O(\epsilon^3)$ terms but all nonlinear terms to this same order.

In this paper, the $O(\epsilon^3)$ differential equations developed in Ref. 4 are used to investigate the influence of these higher-order terms in the elastic response and stability of a rotor blade in the hover flight condition. First, a brief review of the derivation of the equations is given. A small arbitrary ordering-parameter ϵ is then introduced and the equations are simplified by expanding their nonlinearities into a power series in ϵ. The resulting equations are more amenable to analysis, and Galerkin's method is applied to them. After the equilibrium solution to the equations is determined, the blade's elastic deflections are then perturbed about their equilibrium to yield a set of variational equations that are linearized and used to determine the eigenvalues associated with the perturbed motion. The influence of a number of $O(\epsilon^3)$ terms on the blade's response is determined for a range of values of collective pitch.

2. Equations of Motion

2.1 Basic Assumptions and Outline of Derivation

Consider an initially straight rotor blade of closed cross section. Its maximum cross-sectional dimension is assumed to be much smaller than its undeformed length R, so that it may be approximated as a beam. A blade segment, both in its undeformed and deformed states, is shown in Fig. 1. The (η, ζ, ξ) axes shown in the figure, with unit vectors indicated by a *hat* as $\hat{()}$, are the principal axes of the cross section at the shear center C_e of the deformed blade cross section. It is assumed that the cross section is symmetric about the η-axis. The ξ-axis is tangent at all times to the elastic axis of the blade. When the blade is undeformed, the

* Professor, Aerospace Engineering and Applied Mechanics Dept., University of Cincinnati, Cincinnati, Ohio (on academic leave).

** Research Scientist

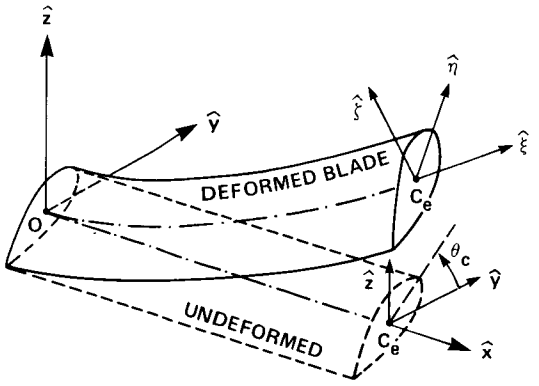

Fig. 1 Undeformed and deformed blade segment with coordinate systems and unit vectors.

principal (η, ζ) axes make an angle θ_c–the collective pitch angle–with the y-axis. The (x, y, z) axes, with unit vectors also indicated by a *hat*, are a set of rotating reference axes as shown in Fig. 2. The x-axis is coincident with the elastic axis of the blade when it is undeformed. These axes are assumed to rotate in space with constant angular velocity Ω about the vertical, which is taken to be perpendicular to the rotor hub. The (X, Y, Z) axes shown in Fig. 2 are a set of inertial axes. The absolute orientation of (x, y, z) may be described by first aligning (x, y, z) with (X, Y, Z) and then performing two successive rotations. The first rotation $\tau = \Omega t$, where t denotes dimensional time, about Z brings the (x, y, z) triad to its new orientation $(X_1, Y_1, Z_1 = Z)$; a second rotation β—the blade's pre-cone angle—about the negative Y_1 direction brings (X_1, Y_1, Z_1) to its "final" orientation (x, y, z). For simplicity, the blade-root offset e_1 shown in Fig. 2 is assumed to be zero.

Because of the elastic deformations, point C_e in Fig. 1 moves from location $(Rx,\ y{=}0,\ z{=}0)$ to $[Rx + Ru(x,\tau), Rv(x,\tau), Rw(x,\tau)]$ relative to the (x, y, z) rotating axes shown in Figs. 1 and 2. Here, (u, v, w) are the components of the elastic displacement vector for C_e, normalized by R. They are functions of the nondimensional variable x–the distance along the x-direction, normalized by R–and of the nondimensional time τ. The orientation of the cross-sectional principal axes (η, ζ, ξ) centered at C_e may be described by a sequence of three-axes Euler angles $(\theta_x = \arctan v'/(1+u'),\ \theta_y = \arcsin w' \partial x/\partial r, \theta_x)$, as described in Refs. 1–4. Here, primes are used to denote partial differentiation with respect to x, and

$$\frac{\partial x}{\partial r} = \left[(1+u')^2 + v'^2 + w'^2\right]^{-\frac{1}{2}} \tag{2.1}$$

The elastic angle of twist of the blade, $\phi(x,\tau)$, is obtained by integrating the torsion of the blade and is related to the Euler angle $\theta_x(x,\tau)$ as[1–4]

$$\phi = \theta_x + \int_0^x \theta_z' \sin\theta_y \, dx \tag{2.2}$$

To obtain the differential equations of motion, and their boundary conditions, use is made of Hamilton's extended principle[5]. These equations were developed in Ref. 4 in terms of the elastic deformations $u(x,\tau)$, $v(x,\tau)$, and $w(x,\tau)$,and of the angle $\theta_x(x,\tau)$. If the blade's mass centroid offset from its elastic axis is neglected, for simplicity, the equations associated with the virtual displacements δu, δv, and δw are of the form

$$\begin{aligned} G_u'(x,\tau) = \ddot{u} - 2\,\dot{v}\cos\beta + w(\sin 2\beta)/2 \\ -(x+u)\cos^2\beta - Q_u \end{aligned} \tag{2.3}$$

$$G_v'(x,\tau) = \ddot{v} + 2\,\dot{u}\cos\beta - 2\,\dot{w}\sin\beta - v - Q_v \tag{2.4}$$

$$\begin{aligned} G_w'(x,\tau) = &\ddot{w} + 2\,\dot{v}\sin\beta + (x+u)(\sin 2\beta)/2 \\ &- w\sin^2\beta - Q_w \end{aligned} \tag{2.5}$$

with the cantilever boundary conditions

$$\begin{aligned} u(0,\tau) = v(0,\tau) = w(0,\tau) \\ = \theta_x(0,\tau) = v'(0,\tau) = w'(0,\tau) = 0 \end{aligned} \tag{2.6}$$

$$G_u(1,\tau) = G_v(1,\tau) = G_w(1,\tau) = \phi'(1,\tau) = 0 \tag{2.7}$$

In the above equations, dots denote differentiation with respect to τ. The G_u, G_v, G_w and G_{θ_x} terms are nonlinear functions of the elastic deformations and of their spatial and temporal derivatives[4]. The Q_u, Q_v, Q_w terms are the distributed forces (normalized by $mR\Omega^2$, where m is the blade's mass per unit length, which is assumed to be constant) associated with the virtual displacements $R\,\delta u$, $R\,\delta v$, and $R\,\delta w$, respectively; and Q_{θ_x} is the distributed moment, normalized by $mR^2\Omega^2$, associated with

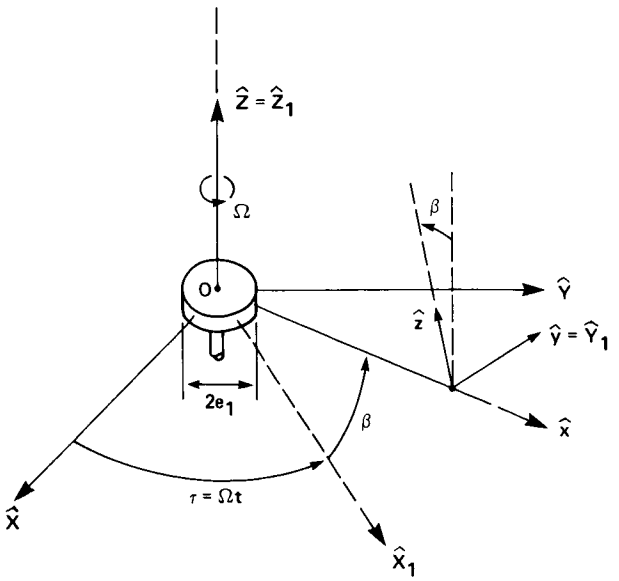

Fig. 2 Nonrotating and rotating coordinate systems with unit vectors.

the virtual rotation $\delta\theta_x$. The normalized virtual work due to these generalized forces is expressed in the form $Q_u\,\delta u + Q_v\,\delta v + Q_w\,\delta w + Q_{\theta_x}\,\delta\theta_x$. The boundary conditions $G_v(1,\tau) = G_w(1,\tau) = 0$ imply $v''(1,\tau) = w''(1,\tau) = v'''(1,\tau) = w'''(1,\tau) = 0$.

For compactness, the fourth differential equation obtained from Hamilton's principle, namely, the equation associated with the virtual rotation $\delta\theta_x$, is presented in the next section in its simplified expanded form only. For its complete form, the reader is referred to Ref. 4.

The aerodynamic forces and moments acting on the blade are modeled using quasi-steady strip theory based on Greenberg's extension of Theodorsen's theory in which only the (η,ς) components of the blade's elastic axis velocity relative to the air are assumed to affect the aerodynamic loading[2,4,6-8]. These components, normalized by the blade's tip speed ΩR, are given as[4]

$$\begin{aligned} U_\eta = T_{22}\,[\,\dot v + (x+u)\cos\beta - w\sin\beta] \\ +T_{23}\,[\,\dot w + v\sin\beta + \lambda\cos\beta] \end{aligned} \tag{2.8}$$

$$\begin{aligned} U_\varsigma = T_{32}\,[\,\dot v + (x+u)\cos\beta - w\sin\beta] \\ +T_{33}\,[\,\dot w + v\sin\beta + \lambda\cos\beta] \end{aligned} \tag{2.9}$$

where,

$$T_{22} = \cos\theta_x\cos\theta_z - \sin\theta_x\sin\theta_y\sin\theta_z \qquad (2.10-a)$$

$$T_{23} = \sin\theta_x\cos\theta_y \qquad (2.10-b)$$

$$T_{32} = -(\sin\theta_x\cos\theta_z + \cos\theta_x\sin\theta_y\sin\theta_z) \qquad (2.10-c)$$

$$T_{33} = \cos\theta_x\cos\theta_y \qquad (2.10-d)$$

and λ is the induced inflow velocity normalized by ΩR.

As shown in Ref. 4, the generalized forces Q_u, Q_v, Q_w, and Q_{θ_x} due to the aerodynamic loading are determined as

$$Q_u = T_{21}F_\eta + T_{31}F_\varsigma - Q_{\theta_x}w'\frac{\partial\theta_x}{\partial u'}\frac{\partial x'}{\partial r} \qquad (2.11-a)$$

$$Q_v = T_{22}F_\eta + T_{32}F_\varsigma - Q_{\theta_x}w'\frac{\partial\theta_x}{\partial u'}\frac{\partial x'}{\partial r} \qquad (2.11-b)$$

$$Q_w = T_{23}F_\eta + T_{33}F_\varsigma \qquad (2.11-c)$$

$$Q_{\theta_x} = -\frac{\gamma}{6}\left[\frac{c^2}{16}(\omega_\xi\sqrt{U_\eta^2+U_\varsigma^2} - \dot U_\varsigma) + 3\frac{c^3}{128}\,\dot\omega_\xi\right] \qquad (2.11-d)$$

with,

$$T_{21} = -(\cos\theta_x\sin\theta_z + \sin\theta_x\sin\theta_y\cos\theta_z) \qquad (2.12-a)$$

$$T_{31} = (\sin\theta_x\sin\theta_z - \cos\theta_x\sin\theta_y\cos\theta_z) \qquad (2.12-b)$$

$$F_\eta = \frac{\gamma}{6}\left[U_\varsigma^2 - \frac{c}{2}U_\varsigma\omega_\xi - \frac{c_{d0}}{2\pi}U_\eta\sqrt{U_\eta^2+U_\varsigma^2}\right] \qquad (2.12-c)$$

$$\begin{aligned} F_\varsigma = \frac{\gamma}{6}\Big[&-U_\eta U_\varsigma + \frac{c}{2}U_\eta\omega_\xi - \frac{c}{4}\dot U_\varsigma + \frac{c^2}{16}\,\dot\omega_\xi \\ &-\frac{c_{d0}}{2\pi}U_\varsigma\sqrt{U_\eta^2+U_\varsigma^2}\Big] \end{aligned} \qquad (2.12-d)$$

In the above equations, c denotes the blade's chord, normalized by R, γ is the Lock number, c_{d0} is the airfoil profile drag coefficient, and ω_ξ is the $\hat\xi$ component of the absolute angular velocity of the principal axis system (η,ς,ξ). It is given as

$$\omega_\xi = \dot\theta_x + (\dot\theta_z + \cos\beta)\sin\theta_y + \sin\beta\cos\theta_y\cos\theta_x \qquad (2.13)$$

In order to compare results with those obtained via the equations developed in Ref. 2, the normalized induced inflow λ is modeled as being uniform along the blade radius and is given as

$$\begin{aligned} \lambda = \mathrm{sgn}\,[\theta_c + \phi_e(0.75)]\,\frac{bc}{8} \\ \left[\sqrt{1+\frac{12}{bc}\,|\,\theta_c + \phi_e(0.75)\,|}\;-1\right] \end{aligned} \tag{2.14}$$

where b is the number of blades, and $\phi_e(0.75)$ is the equilibrium value of the elastic angle of twist at $x = 0.75$.

2.2 Ordering Scheme and Expansion of the Equations to $O(\epsilon^3)$

Because of the complexity of the differential equations presented in the previous section, they will now be restricted to *moderately large* deflections by expanding their nonlinear terms in a Taylor series in a small ordering parameter ϵ, and truncating the result to $O(\epsilon^3)$. Our objective here is to evaluate the influence of these higher-order terms on the motion of the system. We then let $v(x,\tau) = O(\epsilon)$, $w(x,\tau) = O(\epsilon)$ and $\theta_x(x,\tau) = O(\epsilon)$. In addition, $u(x,\tau) = O(\epsilon^2)$. As an example, the expanded form of $\theta_y = \arcsin w'\partial x/\partial r$ is

$$\theta_y = w'(1 - u' - v'^2/2) - w'^3/3 + O(\epsilon^5) \qquad (2.15)$$

By making use of the boundary condition $G_u(1,\tau) = 0$, Eq. (2.3) may be integrated over x to obtain an expression for u' in terms of the remaining variables. With $u(0,\tau) = 0$, the following expression is obtained for $u(x,\tau)$ (Ref. 4)

$$u(x,\tau) = -\frac{1}{2}\int_0^x [v'^2 + w'^2 - \frac{1}{EA}(1-x^2)\cos^2\beta]\,dx - \frac{1}{EA}\int_0^x \int_1^x [2\,\dot{v}\cos\beta + Q_u]\,dx\,dx + O(\epsilon^4)$$
$$\frac{1}{EA} = O(\epsilon^2) \qquad (2.16)$$

where E is the Young's modulus of the material, normalized by $m\Omega^2$, and A is the blade's cross sectional area, normalized by R^2. Both of these quantities are assumed here to be constant.

With u as given by Eq. (2.16), the $O(\epsilon^3)$ expansions for the quantities $G_v(x,\tau)$ and $G_w(x,\tau)$ in the δv and δw equations, Eqs. (2.4) and (2.5), respectively, are now in integro-differential form. Furthermore, since $G_v(1,\tau) = G_w(1,\tau) = 0$, it is convenient to reduce these equations further by integrating them in x from $x = 1$ to $x = x$ and applying the Galerkin procedure to the latter equations. For simplicity, it is also assumed that $\sin\beta = O(\epsilon)$ (with $\cos\beta$ left as an $O(1)$ quantity in the equations), and that $c = O(\epsilon)$, $\lambda = O(\epsilon)$, and $c_{d0} = O(\epsilon^2)$ in the generalized aerodynamic forces.

The expanded $O(\epsilon^3)$ form of the fourth differential equation obtained from Hamilton's principle namely, the equation associated with the virtual rotation $\delta\theta_x$, becomes, after some higher-order cross-sectional integrals are neglected, as is commonly done in the literature (e.g., Refs. 1–4),

$$\begin{aligned}
&\jmath_\xi\left(\ddot{\theta}_x + \underline{\dot{w}'\cos\beta}\right) + (\jmath_\varsigma - \jmath_\eta)\{\underline{\dot{v}'\sin(2\theta_c) - \dot{w}'\cos(2\theta_c)} \\
&\quad + [\theta_x\cos(2\theta_c) + \sin\theta_c\cos\theta_c]\cos\beta\}\cos\beta \\
&\quad - \left\{D_\xi\left[\theta_x' + v''w' - \theta_x'\frac{\cos^2\beta}{EA}(1-x^2)\right]\right. \\
&\qquad \left. + EI_\xi\theta_x'\frac{\cos^2\beta}{EA}(1-x^2)\right\}' \\
&\quad + (D_\eta - D_\varsigma)[\frac{1}{2}\left(v''^2 - w''^2\right)\sin 2(\theta_c+\theta_x) \\
&\qquad - v''w''\cos 2(\theta_c+\theta_x)] \\
&\quad + \frac{\gamma c^2}{96}[x\left(2\,\dot{\theta}_x + \underline{w'\cos\beta} + \underline{\underline{\sin\beta}}\right)\cos\beta\cos\theta_c \\
&\qquad + \underline{\underline{\ddot{v}\sin\theta_c - \ddot{w}\cos\theta_c}}] + O(\epsilon^4) = 0
\end{aligned} \qquad (2.17)$$

All quantities in the above equation are nondimensional. The blade's distributed mass moments of inertia $(\jmath_\eta, \jmath_\varsigma, \jmath_\xi)$ are determined in terms of its material density $\rho(\eta,\varsigma)$ as

$$m\jmath_\eta = R^2\int\int \rho\,\varsigma^2 d\eta\,d\varsigma \qquad (2.18-a)$$

$$m\jmath_\varsigma = R^2\int\int \rho\,\eta^2 d\eta\,d\varsigma \qquad (2.18-b)$$

$$\jmath_\xi = \jmath_\eta + \jmath_\varsigma \qquad (2.18-c)$$

The blade's normalized area moment, I_ξ, is

$$I_\xi = \int\int (\eta^2 + \varsigma^2)d\eta\,d\varsigma \qquad (2.18-d)$$

and $(D_\eta, D_\varsigma, D_\xi)$ are the blade's flexural and torsional normalized stiffnesses determined as

$$D_\eta = E\int\int \varsigma^2\,d_\eta\,d\varsigma \qquad (2.18-d)$$

$$D_\varsigma = E\int\int \eta^2 d_\eta\,d\varsigma \qquad (2.18-e)$$

$$D_\xi = G\int\int [\,(\varsigma + \frac{\partial\psi}{\partial\eta})^2 + (\eta - \frac{\partial\psi}{\partial\varsigma})^2\,]d\eta\,d\varsigma \qquad (2.18-f)$$

where G is the normalized shear modulus of the blade's material and $\psi(\eta,\varsigma)$ is the warp function (normalized by R^2) for the blade's cross section. It is assumed that ψ is anti-symmetric in (η,ς).

For compactness in presentation, two terms in $\sin 2(\theta_c+\theta_x)$ and $\cos 2(\theta_c+\theta_x)$ are shown in Eq. (2.17), but they were actually approximated by their respective expansions to $O(\epsilon^3)$ about $\theta_x = 0$ by writing $\sin 2(\theta_c+\theta_x) = \sin 2\theta_c + 2\theta_x\cos(2\theta_c) + O(\epsilon^2)$ and $\cos 2(\theta_c+\theta_x) = \cos 2\theta_c - 2\theta_x\sin(2\theta_c) + O(\epsilon^2)$. The nonlinear $O(\epsilon^3)$ terms associated with these expansions, namely, the terms in $v''^2\theta_x$, $w''^2\theta_x$ and $v''w''\theta_x$, will henceforth be referred to as the *ijkl terms in the $\delta\theta_x$ equation* in the next figures. The $O(\epsilon^3)$ terms underlined in Eq. (2.17) are not included in the equations developed in Ref. 2. The single underlined terms are linear pitch-flap and pitch-lead/lag coupling terms, and the remaining underlined terms are $O(\epsilon^3)$ linear terms in the aerodynamic pitch moment that are kept for consistency in the formulation. Until a better understanding and more accurate modeling of aerodynamic phenomena is achieved, the validity of terms such as these may be questionable. The $1/(EA)$, $O(\epsilon^3)$, terms in Eq. (2.17) were also neglected in Ref. 2. Again, these terms are kept here for mathematical consistency. For values of EA greater than about 200, we found that the influence of these terms in the results presented later is so small that they may actually be neglected in practice.

2.3 Application of Galerkin's Method

We approximate the solution to Eq. (2.17) and to the integrated form of Eqs. (2.4) and (2.5) as a series of the form

$$v(x,\tau) = \sum_{j=1}^{N} v_{tj}(\tau)\,f_j(x) \qquad (2.19-a)$$

$$w(x,\tau) = \sum_{j=1}^{N} w_{tj}(\tau)\,f_j(x) \qquad (2.19-b)$$

$$\theta_x(x,\tau) = \sum_{j=1}^{N} \theta_{tj}(\tau)\,g_j(x) \qquad (2.19-c)$$

and then reduce the integro-differential equations to ordinary differential equations by making use of Galerkin's method Ref. 5. The functions $f_j(x)$ and $g_j(x)$ are chosen here as the orthogonal eigenfunctions for a nonrotating clamped/free beam,

$$f_j(x) = \cosh(\beta_j x) - \cos(\beta_j x) - \alpha_j\,[\sinh(\beta_j x) - \sin(\beta_j x)] \qquad (2.20-a)$$

$$g_j(x) = \sqrt{2}\sin[\pi(j-\tfrac{1}{2})x] \qquad (2.20-b)$$

where

$$\alpha_j = \frac{\cos\beta_j + \cosh\beta_j}{\sin\beta_j + \sinh\beta_j} \qquad (2.20-c)$$

and β_j is the j^{th} $(j = 1, 2, ..., N)$ root of the characteristic equation

$$1 + (\cosh\beta_j)\cos\beta_j = 0 \qquad (2.20-d)$$

All the *Galerkin coefficients* obtained by the procedure described above were evaluated numerically, stored in a computer file, and then used to generate the results presented in Sections 3 and 4. The ordinary differential equation obtained by applying Galerkin's method to the $\delta\theta_x$ equation is obtained as

$$\begin{aligned}
&\frac{1}{2}(\jmath_\varsigma - \jmath_\eta)Q_i(\sin 2\theta_c)\cos^2\beta + \frac{\gamma c^2}{192}(\sin 2\beta)(\cos\theta_c)\underline{\underline{S_i}} \\
&+\sum_{j=1}^{N}\Big(\,[\jmath_\xi\ddot{\theta}_{tj} + (\jmath_\varsigma - \jmath_\eta)\theta_{tj}(\cos 2\theta_c)\cos^2\beta\,]\delta_{ij} \\
&-[\jmath_\xi\,\dot{w}_{tj} + (\jmath_\varsigma - \jmath_\eta)(\dot{v}_{tj}\sin 2\theta_c - \dot{w}_{tj}\cos 2\theta_c)]\,\underline{L_{3,ji}}\cos\beta \\
&-\Big[D_\xi(P_{ij} + \frac{2\cos^2\beta}{EA}N_{ij}) - \frac{EI_\xi}{EA}N_{ij}\cos^2\beta\Big]\theta_{tj} \\
&+\frac{\gamma c^2}{96}\Big\{(\cos\beta)(\cos\theta_c)\;[2\,\dot{\theta}_{tj}M_{ij} \\
&+(\cos\beta)w_{tj}\underline{\underline{R_{ij}}}] + (\,\tilde{v}_{tj}\sin\theta_c - \tilde{w}_{tj}\cos\theta_c)\underline{\underline{\underline{O_{4,ji}}}}\Big\}\Big) \\
&+\sum_{j=1}^{N}\sum_{k=1}^{N}\Big\{D_\xi A_{3,jik}v_{tj}w_{tk} \\
&+(D_\eta - D_\varsigma)[\,\frac{1}{2}(v_{tj}v_{tk} - w_{tj}w_{tk})\sin 2\theta_c \\
&-v_{tj}w_{tk}\cos 2\theta_c]K_{ijk}\Big\} \\
&+(D_\eta - D_\varsigma)\sum_{j=1}^{N}\sum_{k=1}^{N}\sum_{l=1}^{N}[\,(v_{tj}v_{tk} - w_{tj}w_{tk})\cos 2\theta_c \\
&+2\,v_{tj}w_{tk}\sin 2\theta_c]\theta_{tl}B_{3,jilk} \\
&+O(\epsilon^4) = 0 \qquad (i = 1, 2, ..., N)
\end{aligned} \qquad (2.21)$$

where

$$S_i = \int_0^1 x\,g_i\,dx \qquad (2.22-a)$$

$$R_{ij} = \int_0^1 x\,g_i\,f_j'\,dx \qquad (2.22-b)$$

$$L_{3,ij} = -\int_0^1 f_i' g_j\,dx \qquad (2.22-c)$$

$$O_{4,ij} = \int_0^1 f_i\,g_j\,dx \qquad (2.22-d)$$

$$B_{3,ijkl} = \int_0^1 f_i'' g_j g_k f_l''\,dx \qquad (2.22-e)$$

The terms that are underlined in Eq. (2.21) correspond to those similarly underlined in Eq. (2.17). The $L_{3,ij}$, $O_{4,ij}$, and $B_{3,ijkl}$ Galerkin coefficients also appear in the δv and in the δw equations, with the $L_{3,ij}$ coefficient in the form of a $\dot{\theta}_{tj}$ term. The S_i and R_{ij} coefficients appear only in Eq. (2.21).

3. Equilibrium Solution

3.1 Numerical Method

The differential equations outlined in Section 2 admit the equilibrium solution $v_{tj}(\tau) = \text{constant} = v_{ej}$, $w_{tj}(\tau) = \text{constant} = w_{ej}$, and $\theta_{tj}(\tau) = \text{constant} = \theta_{ej}$. The $3N$ quantities v_{ej}, w_{ej} and θ_{ej}, $j = 1, 2, ..., N$, were determined numerically by solving the algebraic equations obtained from the differential equations in Section 2 using a minimization program[9].

The equilibrium solutions were obtained for a four-bladed rotor with $c = \pi/40$, and using a Lock number $\gamma = 5$, a profile drag coefficient $c_{d0} = 0.01$, and $EA = 200$. The equilibrium deformations at the blade tip, $v_e(x=1)$, $w_e(x=1)$ and $\phi_e(x=1)$ are plotted in Figs. 3 and 4 versus θ_c for $\beta = 0$. The quantities ω_v^*, ω_w^*, and ω_ϕ^* shown in these and in the subsequent figures denote, respectively, the first rotating uncoupled blade natural frequencies normalized by Ω as obtained in Ref. 10. The results shown in these figures were obtained by using $N = 5$ nonrotating beam normal modes in the Galerkin procedure. Greater values of N did not significantly affect the results obtained. The dashed lines shown in Figs. 3 and 4 and in subsequent figures represent the results obtained using the equations in Ref. 2, while the solid lines represent the results obtained when the additional $O(\epsilon^3)$ terms presented here are included in the differential equations of motion. These lines are marked **a**, **b**, **c** and **d** and they represent the following cases:

- **a** the full $O(\epsilon^3)$ equations;
- **b** the $O(\epsilon^3)$ equations, but with $B_{3,ijkl} = 0$;
- **c** the $O(\epsilon^3)$ equations, but with all the $O_{4,ij}$, R_{ij} and $L_{3,ij}$ terms removed, and $B_{3,ijkl} = 0$;
- **d** the $O(\epsilon^3)$ equations, with all the $O_{4,ij}$ and R_{ij} terms removed.

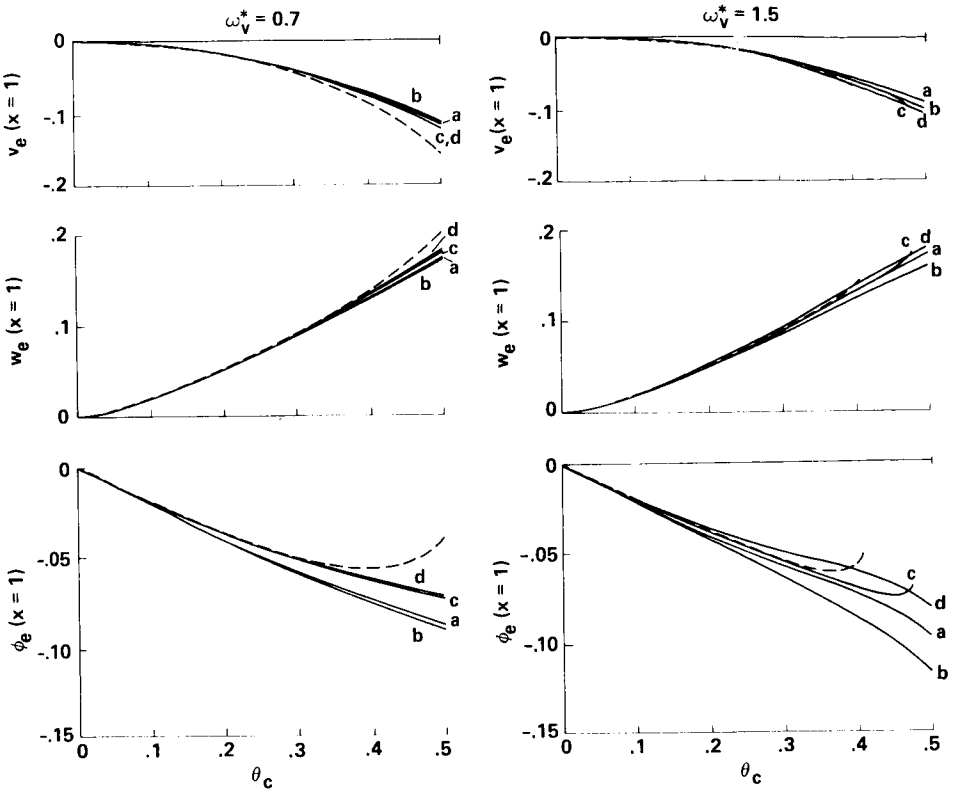

Fig. 3 Chordwise deflection (v_e), flapwise deflection (w_e), and angle of twist (ϕ_e) at $x = 1$ versus collective pitch (θ_c) for $\omega_w^* = 1.06$, $\beta = 0$, $\omega_\phi^* = 2.5$, (N = 5).

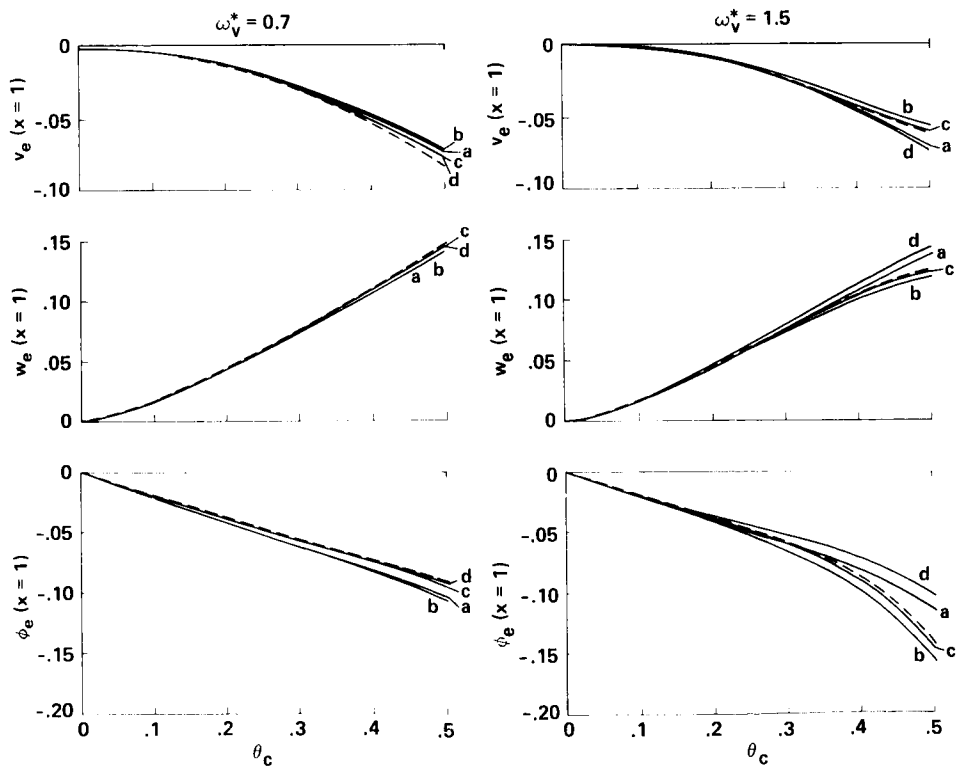

Fig. 4 Chordwise deflection (v_e), flapwise deflection (w_e), and angle of twist (ϕ_e) at $x = 1$ versus collective pitch (θ_c) for $\omega_w^* = 1.15$, $\beta = 0$, $\omega_\phi^* = 2.5$, (N = 5).

3.2 Discussion of Results

Figs. 3 and 4 illustrate the importance of the $O(\epsilon^3)$ terms of the type underlined in Eq. (2.21) in the equilibrium solution of the blade. Their effect is particularly reflected in the equilibrium value of the blade's angle of twist, $\phi_e(x = 1)$, especially for the lower value of the uncoupled flap frequency $\omega_w^* = 1.06$. Several of the nonlinear terms may have only a minor influence on the blade's equilibrium deflections. For soft in-plane blades with $\omega_v^* = 0.7$, for example, it is seen that the equilibrium curves **a** and **b** are nearly identical; the same is true of curves **c** and **d**. This indicates that for such blades, the additional aerodynamic $O(\epsilon^3)$ terms of the type indicated in Eq. (2.21) are essentially responsible for the difference between curve **a** and the remaining curves. For these blades, the nonlinear $B_{3,ijkl}$ terms in Eq. (2.21) could have been neglected without causing any significant change in the blade's equilibrium deflections. For high values of collective pitch, however, those terms exert a significant influence on the blade's equilibrium, affecting especially its elastic angle of twist.

Another characteristic of the full $O(\epsilon^3)$ equations is disclosed by examining the equilibrium response of a stiff in-plane blade with $\omega_w^* = 1.06$. The numerical determination of the equilibrium deflections based on the equations developed in Ref. 2 fails to converge when θ_c is about 0.4. This *singularity* is shifted to a higher value of θ_c when additional $O(\epsilon^3)$ terms are included in the equations. For the full $O(\epsilon^3)$ nonlinear equations, no singularity is exhibited in the range of θ_c shown in Figs. 3 and 4. If the aerodynamic $O_{4,ij}$ and R_{ij} terms and the $B_{3,ijkl}$ terms are neglected, but if all other additional terms in the equations are kept, the singularity now appears near $\theta_c = 0.5$.

It was verified that the $O(\epsilon^3)$ *ijkl terms in the* δv and δw *equations*, did not contribute significantly to the determination of the blade's equilibrium response and, therefore, could have been neglected for practical purposes.

4. Stability Analysis

4.1 Numerical Method

To analyze the stability of the motion about the equilibrium determined in Section 3, we let

$$v_{tj}(\tau) = v_{ej} + v_j(\tau) \qquad (4.1-a)$$

$$w_{tj}(\tau) = w_{ej} + w_j(\tau) \qquad (4.1-b)$$

$$\theta_{tj}(\tau) = \theta_{ej} + \theta_j(\tau) \qquad (4.1-c)$$

and then linearize the $3N$ differential equations of motion in the variables $v_j(\tau)$, $w_j(\tau)$, and $\theta_j(\tau)$ to obtain a matrix equation of the form

$$M\underline{\ddot{q}} + C\,\underline{\dot{q}} + K\underline{q} = \underline{0} \qquad (4.2)$$

where $\underline{q}$ is a $3N \times 1$ column vector whose components are $v_1(\tau)$, ... , $v_N(\tau)$, $w_1(\tau)$, ... , $w_N(\tau)$, $\theta_1(\tau)$, ... , $\theta_N(\tau)$. The matrix M is symmetric, and the matrices K and C are non-symmetric.

The stability of the perturbed motion $\underline{q}(\tau)$ is determined by the eigenvalues associated with Eq. (4.2). To determine such eigenvalues, Eq. (4.2) is first rewritten in a first-order form. After introduction of a column vector $\underline{z}$ with components $\underline{q}$ and $\underline{\dot{q}}$, Eq. (4.2) may be written as

$$B\,\underline{\dot{z}} = A\underline{z} \qquad (4.3)$$

with $B_{11} = I$, a $3N \times 3N$ identity matrix; $B_{12} = B_{21} = [0]$; a $3N \times 3N$ null matrix; $B_{22} = M$; $A_{11} = [0]$; $A_{12} = I$; $A_{21} = -K$; and $A_{22} = -C$. The eigenvalues associated with the $6N \times 6N$ matrix in Eq. (4.3) were determined numerically by making use of the IMSL routine EIGZF[9].

The real and imaginary parts of the first lead/lag (σ_v and ω_v), first flap (σ_w and ω_w), and first torsion (σ_ϕ and ω_ϕ) eigenvalues determined as indicated above are plotted versus collective pitch (θ_c) in Figs. 5 to 10 using the same parameter values and labeling convention indicated in Section 3.1.

4.2 Discussion of Results

Figs. 5 and 6 show the first lead/lag eigenvalue associated with Eq. (4.3) for the rotating blade as a function of the pitch angle θ_c. It is seen that for a soft in-plane blade with uncoupled rotating natural frequency $\omega_v^* = 0.7$ the nonlinear $O(\epsilon^3)$ $B_{3,ijkl}$ term that appear in Eq. (2.21) has no substantial influence on either σ_v or ω_v. For such blades, the influence of the remaining higher-order terms underlined in Eq. (2.21) is reflected in the difference between curve **d** (i.e., with the aerodynamic terms $O_{4,ij}$ and R_{ij} removed from the equations) and that obtained with the full $O(\epsilon^3)$ equations (curve **a**), and curves **a** and **c** (i.e., with the $L_{3,ij}$ torsion-bending coupling terms, and the $O_{4,ij}$ and R_{ij} aerodynamic terms removed from the full $O(\epsilon^3)$ equations). The additional $O(\epsilon^3)$ terms included in the δv and δw equations account for the difference between the results obtained by using the equations developed in Ref. 2—represented by the dashed line—and those represented by curves **a** in Figs. 5 and 6.

As ω_v^* is increased, however, the situation described above changes. For a stiff in-plane blade with $\omega_v^* = 1.5$, the nonlinear $B_{3,ijkl}$ term that appears in Eq. (2.21) now exerts a major influence on the real part σ_v of the first rotating lead/lag eigenvalue, whereas the terms in the underlined coefficients in Eq. (2.21) do not. The effect of the $O(\epsilon^3)$ nonlinearities that appear in the δv and δw equations is seen by comparing curve **c** with the dashed curve obtained by using the equations in Ref. 2. For values of θ_c as high as about 0.4, the latter equations yield, for this stiff in-plane blade, practically the same values for ω_v as the full $O(\epsilon^3)$ equations used in this paper. At about $\theta_c = 0.4$, the numerical calculation of the eigenvalues based on the equations in Ref. 2 fail to converge.

The first flap eigenvalue obtained from Eq. (4.3) is shown in Figs. 7 and 8. Again, the effect of $B_{3,ijkl}$ on both σ_w and ω_w is negligible for a soft in-plane blade with $\omega_v^* = 0.7$, but significant for a stiff in-plane blade with $\omega_v^* = 1.5$ for higher values of collective pitch. The effect of the apparent inertia, $O_{4,ij}$, and of the R_{ij} aerodynamic terms, generally neglected in the literature, is reflected in

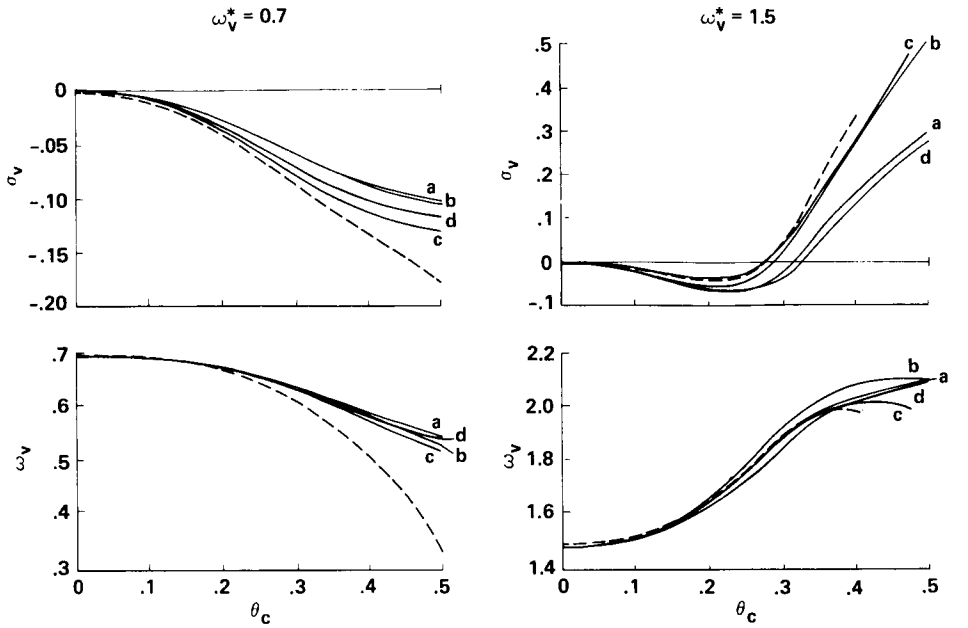

Fig. 5 First lead/lag eigenvalues (real part, σ_v, and imaginary part, ω_v) versus collective pitch (θ_C) for $\omega_w^* = 1.06$, $\beta = 0$, $\omega_\phi^* = 2.5$, (N = 5).

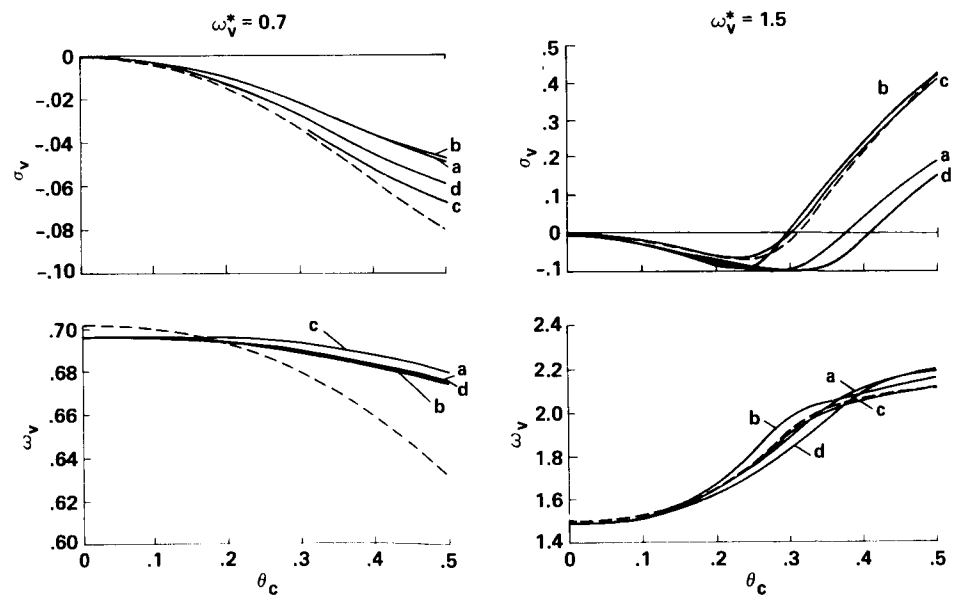

Fig. 6 First lead/lag eigenvalues (real part, σ_v, and imaginary part, ω_v) versus collective pitch (θ_C) for $\omega_w^* = 1.15$, $\beta = 0$, $\omega_\phi^* = 2.5$, (N = 5).

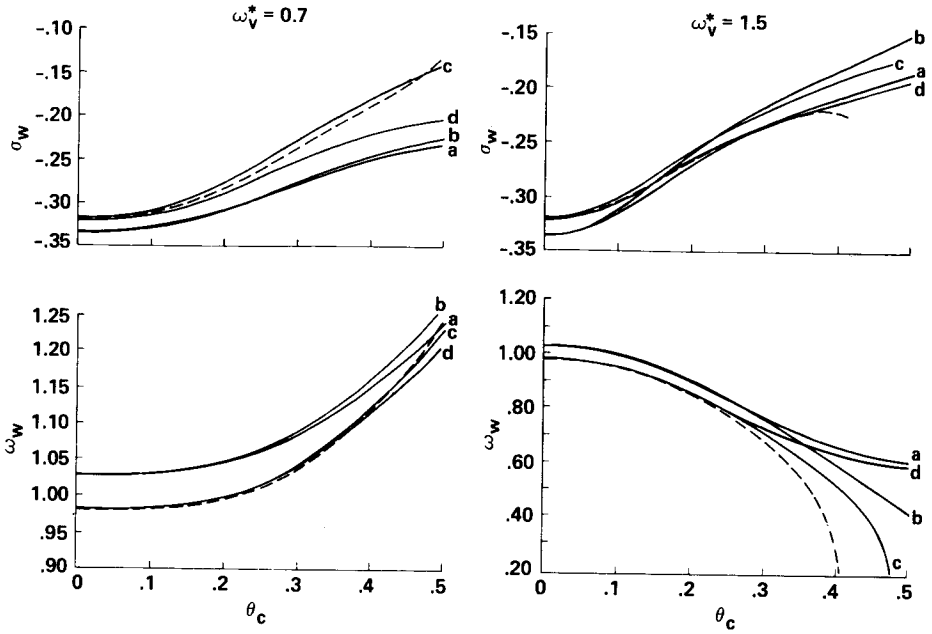

Fig. 7 First flap eigenvalues (real part, σ_w, and imaginary part, ω_w) versus collective pitch (θ_c) for $\omega_w^* = 1.06$, $\beta = 0$, $\omega_\phi^* = 2.5$, (N = 5).

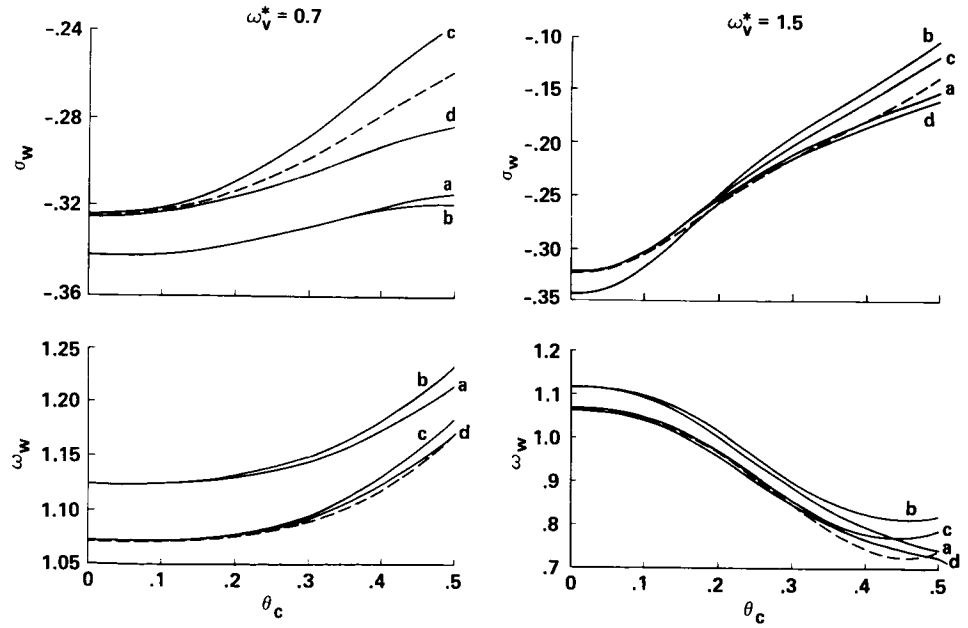

Fig. 8 First flap eigenvalues (real part, σ_w, and imaginary part, ω_w) versus collective pitch (θ_c) for $\omega_w^* = 1.15$, $\beta = 0$, $\omega_\phi^* = 2.5$, (N = 5).

the eigenvalue (σ_w, ω_w) even for $\theta_c = 0$. It was verified numerically that the $L_{3,ij}$ torsion-bending coupling term that appears in Eq. (2.21)—and also in the δv and δw variational equations as a $\dot{\theta}_j$ term—has no practical influence on ω_w. Its influence on σ_w was found to be negligible for $\omega_v^* = 1.5$, but significant when $\omega_v^* = 0.7$. As indicated by Figs. 7 and 8, the damping for the perturbed flap motion for a soft in-plane blade can be significantly affected by the additional $O(\epsilon^3)$ terms included in the equations used here.

Figs. 9 and 10 show the real and imaginary parts of the first rotating torsion eigenvalues of Eq. (4.3). The values of the torsional frequency ω_ϕ are relatively large, and, as seen from these figures, there is little difference between the results obtained here and those obtained by using the equations in Ref. 2 for small values of θ_c. For larger values of collective pitch θ_c, however, the full $O(\epsilon^3)$ equations used here and those in Ref. 2 predict a different trend for ω_ϕ as θ_c is increased further. However, this trend difference is

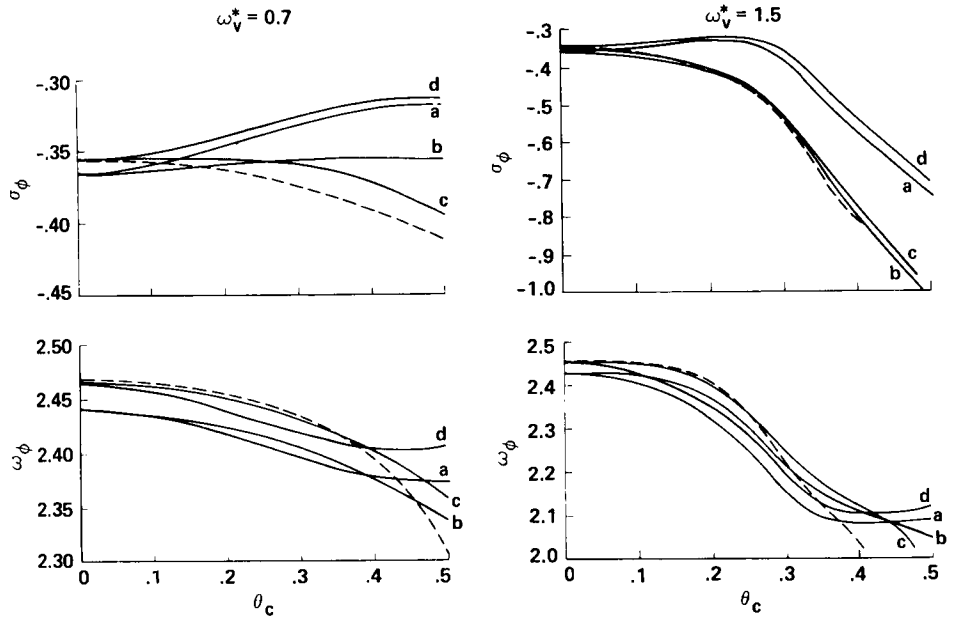

Fig. 9 First torsion eigenvalues (real part, σ_ϕ, and imaginary part, ω_ϕ) versus collective pitch (θ_c) for $\omega_w^* = 1.06$, $\beta = 0$, $\omega_\phi^* = 2.5$, (N = 5).

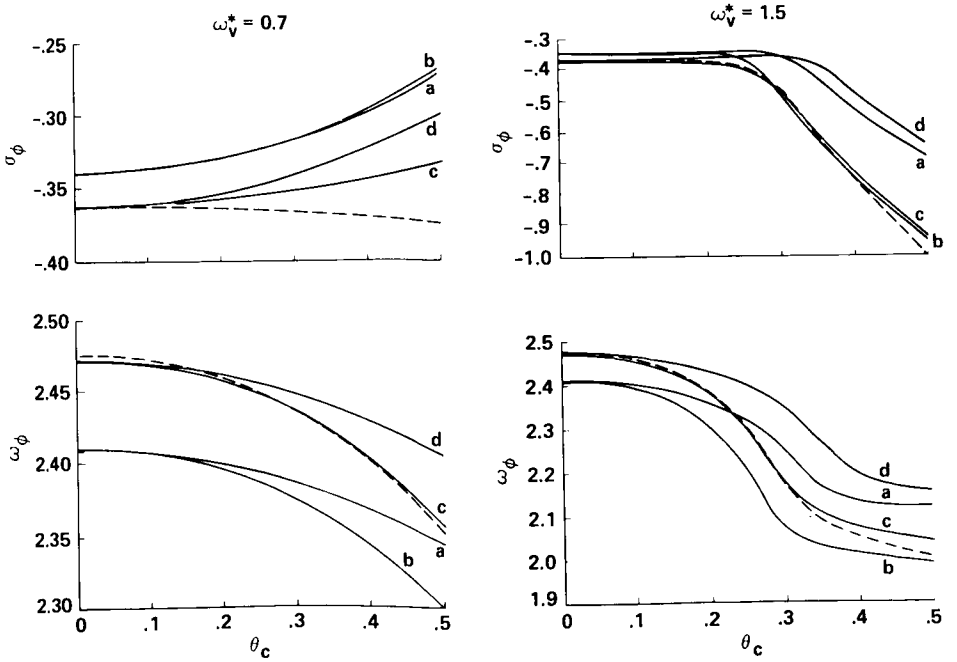

Fig. 10 First torsion eigenvalues (real part, σ_ϕ, and imaginary part, ω_ϕ) versus collective pitch (θ_c) for $\omega_w^* = 1.15$, $\beta = 0$, $\omega_\phi^* = 2.5$, (N = 5).

exhibited at such high values of θ_c that it may not be of practical significance.

The torsion damping is significantly affected by the $O(\epsilon^3)$ terms included in the equations used in this paper. Particularly noticeable in Figs. 9 and 10 is the opposing torsion damping trends for a soft in-plane blade with $\omega_\nu^* = 0.7$ for increasing values of θ_c. This is observed by comparing the results given by curve a, obtained with the full $O(\epsilon^3)$ equations, and by the dashed curve obtained by using the equations in Ref. 2.

It is worth mentioning that all the results shown in Figs. 3 to 10 were essentially unaffected by the $O(\epsilon^3)$ *ijkl terms in the* δv and δw *equations.* These are terms in $v_{tj}w_{tk}\theta_{tl}$, $v_{tj}\dot{w}_k\theta_{tl}$, etc.

5. Concluding Remarks

Numerical results obtained from nonlinear rotor blade equations for the hovering flight condition, with terms retained up through $O(\epsilon^3)$, are presented and compared with results from a simpler $O(\epsilon^2)$ model obtained by previous investigators[2]. In order to facilitate an understanding of which terms are important in the present model that were absent in the previous, simpler model, the present model was exercised with several different classes of terms systematically omitted. Present results, a subset of all the results obtained, indicate that both linear and nonlinear terms of $O(\epsilon^3)$ can significantly affect results for both nonlinear static equilibrium and linear aeroelastic stability. For the results presented here, the most significant cubic nonlinear terms are those associated with structural geometric nonlinearity in the torsion equation. It would appear that such terms should be present in any general-purpose rotor dynamics analysis. The corresponding terms in the equations for bending, although not practically significant in the present results, do make the structural terms in the equations symmetric. The most significant linear terms in the present model but absent in Ref. 2 are associated with an approximate aerodynamics model, the accuracy of which has not been rigorously ascertained. For completeness, it is recommended that a similar investigation be undertaken for the forward flight condition to determine if similar trends hold.

6. References

1. Hodges, D. H. and Dowell, E. H., "Nonlinear Equations of Motion for the Elastic Bending and Torsion of Twisted Nonuniform Blades," NASA TN D-7818, December 1974.

2. Hodges, D. H. and Ormiston, R. A., "Stability of Elastic Bending and Torsion of Uniform Cantilever Rotor Blades in Hover with Variable Structural Coupling," NASA TN D-8192, April 1976.

3. Crespo da Silva, M. R. M. and Glynn, C. C., "Nonlinear Flexural-Flexural-Torsional Dynamics of Inextensional Beams. I. : Equations of Motion; and II. Forced Motion," *J. Structural Mech.*, Vol. 6, No. 4, 1978, pp. 437-448; 449-461.

4. Crespo da Silva, M. R. M., "Flap-Lag-Torsional Dynamic Modeling of Rotor Blades in Hover and in Forward Flight, Including the Effect of Cubic Non-linearities," NASA CR-166194, July 1981.

5. Meirovitch, L., *Analytical Methods in Vibrations.* McGraw Hill, New York, N.Y., 1967.

6. Bisplinghoff, R. L., Ashley, H., and Halfman, R. L., *Aeroelasticity.* Addison-Wesley, 1955.

7. Greenberg, J. M., "Airfoil in Sinusoidal Motion in a Pulsating Stream," NASA TN-1326, 1946.

8. Theodorsen, T., "General Theory of Aerodynamic Instabilities and the Mechanism of Flutter," NACA Report No. 496, 1935.

9. *The International Mathematical and Statistical Library,* Vol. 4, Chapter Z, IMSL Inc., Houston, Texas, 1982.

10. Peters, D. A., "An Approximate Solution for the Free Vibrations of Rotating Uniform Cantilever Beams," NASA TM X-62,299, 1973.